Biochemical Pharmacology 82 (2011) 842–851

Contents lists available at ScienceDirect

Biochemical Pharmacology

journal homepage: www.elsevier.com/locate/biochempharm

# Endogenous activation of nAChRs and NMDA receptors contributes to the excitability of CA1 stratum radiatum interneurons in rat hippocampal slices: Effects of kynurenic acid

Manickavasagom Alkondon, Edna F.R. Pereira, Edson X. Albuquerque *

*Division of Translational Toxicology, Department of Epidemiology and Public Health, University of Maryland School of Medicine, 10 S. Pine Street, Suite 900, Baltimore, MD 21201, United States*

ARTICLE INFO

*Article history:*
Received 2 May 2011
Accepted 2 June 2011
Available online 13 June 2011

*Keywords:*
Action potential
Nicotinic receptor
NMDA receptor
Kynurenic acid
Hippocampus
Mecamylamine

ABSTRACT

CA1 stratum radiatum interneurons (SRIs) express α7 nicotinic receptors (nAChRs) and receive inputs from glutamatergic neurons/axons that express α3β4β2 nAChRs. To test the hypothesis that endogenously active α7 and/or α3β4β2 nAChRs control the excitability of CA1 SRIs in the rat hippocampus, we examined the effects of selective receptor antagonists on spontaneous fast current transients (CTs) recorded from these interneurons under cell-attached configuration. The frequency of CTs, which represent action potentials, increased in the absence of extracellular $Mg^{2+}$ and decreased in the presence of the α3β4β2 nAChR antagonist mecamylamine (3 μM) or the NMDA receptor antagonist APV (50 μM). However, it was unaffected by the α7 nAChR antagonist MLA (10 nM) or the AMPA receptor antagonist CNQX (10 μM). Thus, in addition to synaptically and tonically activated NMDA receptors, α3β4β2 nAChRs that are present on glutamatergic axons/neurons synapsing onto SRIs and are activated by basal levels of acetylcholine contribute to the maintenance of the excitability of these interneurons. Kynurenic acid (KYNA), an astrocyte-derived kynurenine metabolite whose levels are increased in the brains of patients with schizophrenia, also controls the excitability of SRIs. At high micromolar concentrations, KYNA, acting primarily as an NMDA receptor antagonist, decreased the CT frequency recorded from the interneurons. At 2 μM, KYNA reduced the CA1 SRI excitability via mechanisms independent of NMDA receptor block. KYNA-induced reduction of excitability of SRIs may contribute to sensory gating deficits that have been attributed to deficient hippocampal GABAergic transmission and high levels of KYNA in the brain of patients with schizophrenia.



## 1. Introduction

Cholinergic innervation of hippocampal neurons is known to play an important role in a variety of cognitive processes. In fact, several lines of evidence have suggested that impairment of hippocampal inhibitory neurotransmission due to deficits in cholinergic stimulation of hippocampal interneurons contributes to the over-inclusive thought processing of patients with schizophrenia [1]. In this disorder, impaired cholinergic stimulation of GABAergic neurons in the hippocampus may result from elevated levels of kynurenic acid (KYNA) [2], an astrocyte-derived kynurenine metabolite known to block both NMDA receptors and α7 nicotinic acetylcholine receptors (nAChRs) [3–6].

Interneurons in the hippocampus receive cholinergic inputs from the medial septal nucleus/diagonal band complex [7] and from cholinergic neurons intrinsic to the hippocampal formation [8,9]. It is well documented that the excitability of the interneurons is controlled by interactions of endogenously released acetylcholine (ACh) with different subtypes of muscarinic receptors present in the local interneuronal circuitry and on glutamatergic axons/neurons that synapse onto the interneurons [10,11]. By contrast, much less is known regarding control of neuronal excitability in the hippocampus by the actions of the endogenous neurotransmitter, ACh, on nicotinic receptors (nAChRs). Two independent studies reported the existence of nicotinic synaptic transmission mediated by α7 nAChRs on a small population of CA1 stratum radiatum interneurons (SRIs) [12,13]. Evoked release of ACh in hippocampal slices has also been shown to cause α7 nAChR-dependent heterosynaptic depression of GABAergic transmission in interneurons [14]. However, exogenous application of nicotinic agonists to hippocampal interneurons led to the identification of

*Abbreviations:* ACh, acetylcholine; ACSF, artificial cerebrospinal fluid; AMPA, (2R)-amino-5-phosphonovaleric acid; CNQX, 6-cyano-7-nitroquinoxaline-2,3-dione; CT, current transient; EPSC, excitatory postsynaptic current; KYNA, kynurenic acid; MLA, methyllycaconitine; nAChR, nicotinic acetylcholine receptor; SRI, stratum radiatum interneuron.

* Corresponding author. Tel.:+1 410 706 7065; fax: +1 410 706 4200.
*E-mail address:* ealbuque@umaryland.edu (E.X. Albuquerque).

0006-2952/$ – see front matter © 2011 Published by Elsevier Inc.
doi:10.1016/j.bcp.2011.06.004

neuron-type specific expression of pharmacologically distinct nAChR subtypes [15]. For instance, exogenous application of ACh and other nicotinic agonists to the majority of CA1 SRIs in rat hippocampal slices induces responses that have the pharmacological profile of α7 nAChR [16–19]. However, these neurons also receive glutamatergic inputs whose activity is increased by α3β4β2 nAChRs [20] and GABAergic inputs whose activity is regulated by α7 nAChRs and α4β2 nAChRs [17]. Therefore, one can hypothesize that nicotinic cholinergic regulation of the excitability of CA1 SRIs is a result of the interactions of endogenous ACh with: (i) α7 nAChRs present on the somatodendritic region of SRIs, (ii) α3β4β2 nAChRs present on glutamatergic neurons/axons synapsing onto the SRIs, and (iii) α7 and α4β2 nAChRs present on interneurons that synapse onto the SRIs. The present study was designed to address specifically the contribution of α7 and α3β4β2 nAChR activation by endogenous ACh to the resting excitability of CA1 SRIs.

Action potentials, the output signal of neurons, are commonly studied in intracellular or whole-cell current-clamp recordings performed in brain slices [21,22]. In a few studies, action potentials have been detected as fast current transients (CTs) in single neurons under cell-attached voltage-clamped condition [23,24]. Under voltage-clamp, these fast CTs appear as inverted action potentials. A pharmacological analysis of spontaneous CTs in identified neuron types in brain slices can underpin the contribution of specific neurotransmitter systems to the regulation of neuronal excitability [21,22]. Thus, here, to identify how endogenously activated nAChRs and glutamate receptors control the excitability of CA1 SRIs, receptor-subtype selective antagonists were applied to rat hippocampal slices where fast CTs were recorded from the interneurons under voltage-clamp cell-attached configuration. Specifically, we analyzed the effects of the α7 nAChR antagonist methyllycaconitine (MLA), the NMDA receptor antagonist (2R)-amino-5-phosphonovaleric acid (APV), and the AMPA receptor antagonist 6-cyano-7-nitroquinoxaline-2,3-dione (CNQX) on the frequency of CTs. The effects of a concentration of mecamylamine that selectively inhibits α3β4β2 nAChRs were also analyzed. Finally, we examined whether the frequency of CTs recorded from SRIs is affected by endogenously produced and exogenously applied KYNA.

## 2. Methods

### 2.1. Animals

Timed pregnant rats (Sprague–Dawley, gestation day 16–18) were purchased from Charles River Laboratories (Wilmington, MA) and housed individually in a temperature- and light-controlled animal-care unit. Male pups were weaned at 21 days of age and housed in groups of three–four per cage and used for experiments on postnatal days 23–30. Animals were handled according to the regulations of the Association for Assessment and Accreditation of Laboratory Animal Care, in compliance with the standards of the Animal Welfare Act and in adherence to the principles of the '1996 Guide for the Care and Use of Laboratory Animals.'

### 2.2. Hippocampal slices

Rats were euthanized by asphyxiation in a $CO_2$ atmosphere followed by decapitation using a guillotine. To reduce cell swelling, removal of the brains as well as dissection and slicing of the hippocampi were performed in an ice-cold solution consisting of a mixture of equal parts of regular artificial cerebrospinal fluid (ACSF) and sucrose-containing ACSF. Regular ACSF (Mg-ACSF) was composed of (in mM): NaCl, 125; $NaHCO_3$, 26; KCl, 2.5; $NaH_2PO_4$, 1.25; $CaCl_2$, 2; $MgCl_2$, 1; and glucose, 25. Nominally $Mg^{2+}$-free ACSF had the same composition but $MgCl_2$ was excluded. Sucrose-containing ACSF was composed of (in mM): sucrose, 230; KCl, 2.5; $NaH_2PO_4$, 1.25; $NaHCO_3$, 26; $CaCl_2$, 0.5; $MgSO_4$, 10; and glucose, 10. Hippocampal slices of 300-μm thickness were cut using the vibratome Leica VT1000S (Leica Microsystems Inc., Bannockburn, IL) and transferred to an immersion chamber containing regular ACSF that was continuously bubbled with 95% $O_2$/5% $CO_2$. After 30 min incubation in regular ACSF, 12 hippocampal slices were transferred to a 50-ml chamber containing ACSF, with test compounds, that was continuously bubbled with 95% $O_2$/5% $CO_2$. The chambers were maintained in a water bath at 30 °C. Time of incubation of the slices with the test compounds ranged from 1 to 6 h.

### 2.3. Electrophysiological recordings

Hippocampal slices were transferred to a 1-ml recording chamber, where they were continuously superfused with ACSF at 2 ml/min at room temperature. In all experiments, ACSF used to superfuse the slices contained the muscarinic antagonist atropine (0.5 μM) and $GABA_A$ receptor antagonist bicuculline (10 μM). Cell-attached and whole-cell recordings were obtained from the soma of SRIs in hippocampal slices according to the standard patch-clamp technique using an EPC9 amplifier (HEKA Elektronik, Lambrecht, Germany).

Signals were filtered at 3 kHz and either videotape recorded for later analysis or directly sampled by a microcomputer using the PULSE software (ALA Scientific Instruments, Inc., Westbury, NY). Patch pipettes were pulled from a borosilicate glass capillary (1.2-mm OD) that, when filled with internal solution, had resistances between 3 and 5 MΩ. The internal pipette solution contained 0.5% biocytin in addition to ethylene-glycol bis (β-amino-ethyl ether)-N-N′-tetraacetic acid, 10 mM; 4-(2-hydroxyethyl)-1-piperazineethanesulfonic acid, 10 mM; Cs-methane sulfonate, 130 mM; CsCl, 10 mM; $MgCl_2$, 2 mM (pH adjusted to 7.3 with CsOH; 340 mOsm). To record AMPA or NMDA EPSCs from neurons under whole-cell configuration, 5 mM N-(2,6-dimethylphenyl-carbamoylmethyl)triethylammonium bromide (QX314) was included in the pipette solution. QX314 – free pipette solution was used for all cell-attached recordings, except those that preceded whole-cell recordings from a single neuron. CTs were recorded in the cell-attached mode after formation of the seal, which ranged between 1 and 8 GΩ in our recordings. During cell-attached recordings the patch pipette was held at −60 mV (i.e., transmembrane potential close to 0 mV) to inactivate voltage-dependent currents [23]. All experiments were carried out at room temperature (20–22 °C).

### 2.4. Data analysis

The frequency of CTs was analyzed using the pCLAMP9 software (Molecular Devices, Sunnyvale, CA). Frequency, peak amplitude, 10–90% rise time, and decay-time constants of α-amino-3-hydroxy-5-methyl-4-isoxazolepropionic acid (AMPA) excitatory PSCs (EPSCs) were analyzed using WinEDR V2.3 and WinWCP 4.2.8 (Strathclyde Electrophysiology Software, Glasgow, Scotland). Results are presented as mean ± SEM. Statistical significance was tested with the StatsDirect software v 2.7.7 (StatsDirect Ltd., Cheshire, UK) using unpaired t-test, Fisher's exact test, or one-way ANOVA followed by an appropriate post-hoc test.

### 2.5. Chemicals used

(−)Bicuculline methochloride was purchased from Tocris (Ellisville, MO). Atropine sulfate, L-kynurenine sulfate, KYNA, QX-314 bromide, and 2-amino-5-phosphonovaleric acid (APV)

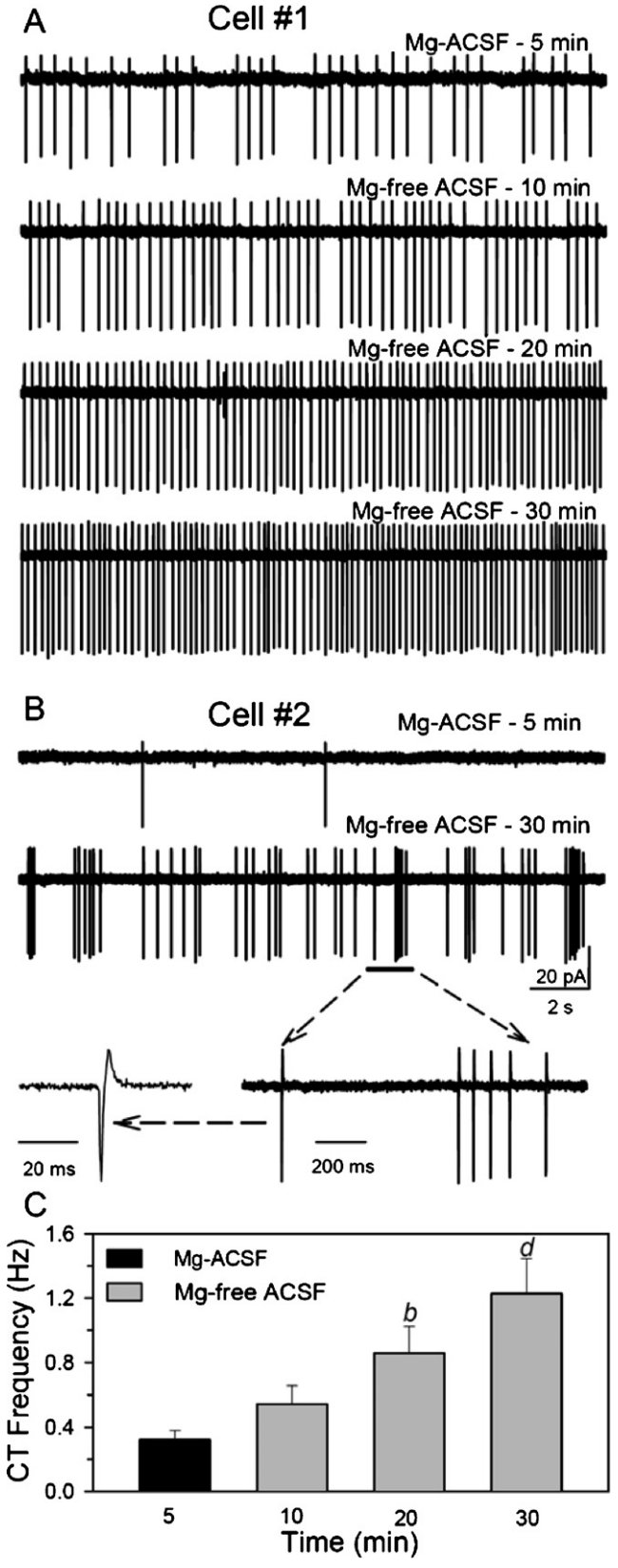


**Fig. 1.** Pattern of firing of CA1 SRIs in rat hippocampal slices. Samples of current transients (CTs) recorded from an SRI using cell-attached configuration. All recordings were performed in the voltage-clamp mode at −60 mV in the continuous presence of the $GABA_A$ receptor antagonist bicuculline (10 μM) and the muscarinic receptor antagonist atropine (0.5 μM). A. Segments (20-s each) of recordings obtained from an SRI under various conditions are shown. In the nominal absence of extracellular $Mg^{2+}$, the firing rate of the SRI increased. This pattern illustrates the presence of non-overlapping CTs even during high-frequency firing. B. Segments of recordings obtained from another SRI under two different ACSF conditions. This pattern illustrates the presence of both isolated events and bursts of CTs as revealed in the expanded traces. Single CT shown at the bottom reveals a fast inward component and a slow outward component that resembles the components of an action potential in extracellular recordings [22,23]. C. Graph shows CT frequency recorded from several neurons in $Mg^{2+}$-containing ACSF during 10 min and after exposure to $Mg^{2+}$-free ACSF. In $Mg^{2+}$-free ACSF, 5 min recording segments (i.e., 5–10, 15–20, and 25–30 min) were used for the analysis. Graph and error bars represent mean and S.E.M. of results from 92 neurons in $Mg^{2+}$-containing ACSF and 58 neurons in $Mg^{2+}$-free ACSF. b $p < 0.01$; d $p < 0.0001$ compared to $Mg^{2+}$-ACSF by one-way ANOVA followed by Bonferroni comparison.

**Table 1**
Incidence of SRI CTs among different treatment groups.

| Treatment groups | # of neurons studied | # of CT-positive neurons (% CT positive) |
|---|---|---|
| Control ACSF | 95 | 68 (71.5%) |
| MLA, 10 nM | 13 | 7 (53.8%) |
| Mecamylamine, 3 μM | 9 | 4 (44.4%) |
| CNQX, 10 μM | 13 | 6 (46.1%) |
| APV, 50 μM | 9 | 2 (22.2%)** |
| KYNA, 2 μM | 12 | 1 (8.3%)*** |
| Kynurenine, 200 μM | 22 | 10 (45.4%)* |

In all groups, current transients (CT) were recorded in $Mg^{2+}$-ACSF for 10 min after obtaining cell-attached configuration. Hippocampal slices were incubated in control ACSF or ACSF containing test drugs for >1 h before recordings started. Same concentrations of test drugs were present in the ACSF during the recordings. Other groups were not significantly different from control.
* $p < 0.02$ compared to control group by Fisher's exact test.
** $p < 0.01$ compared to control group by Fisher's exact test.
*** $p < 0.0001$ compared to control group by Fisher's exact test.

were purchased from Sigma Chemical Co. (St. Louis, MO). 6-cyano-7-nitroquinoxalene-2,3-dione (CNQX) was purchased from Research Biochemicals (Natick, MA). Methyllycaconitine citrate (MLA) was a gift from Professor M.H. Benn (Dept. Chemistry, Univ. Calgary, Alberta, Canada). (±)Mecamylamine hydrochloride was a gift from Merck Research Laboratories (Rathway, NJ).

## 3. Results

### 3.1. Pattern of spontaneous firing in CA1 SRI of control hippocampal slices

Spontaneous CTs were recorded from CA1 SRIs under cell-attached, voltage-clamp configuration at −60 mV. All experiments were conducted in the presence of 10 μM bicuculline and 0.5 μM atropine to remove the contribution of $GABA_A$ inhibition and muscarinic receptor activity, respectively, to the activity of the neurocircuitry.

Individual CTs had a fast inward component and a large slow outward component (see expanded single event in Fig. 1B) and represented action potentials recorded under voltage-clamp [22,23]. In the cell-attached mode, the frequency of CTs could be evaluated in intact SRIs without the problems of dialysis and subsequent loss of intracellular contents associated with conventional whole-cell recordings.

In $Mg^{2+}$-containing ACSF, spontaneous CTs were recorded from 71% of the SRIs studied. No CT was detected during the recording period (~10 min) in the remaining 29% neurons (Table 1). Under this experimental condition, the frequency of CTs was 0.321 ± 0.055 Hz, ranging from 0 to 2.60 Hz ($n = 92$ neurons). When the slices were subsequently superfused with $Mg^{2+}$-free ACSF, the frequency of CTs increased in a time-dependent manner during a 30-min recording session (Fig. 1A and C). The frequency of CTs was nearly four-fold higher at 30 min of superfusion with $Mg^{2+}$-free ACSF than at 5-min superfusion with $Mg^{2+}$-containing ACSF (Fig. 1C). Further, in $Mg^{2+}$-free ACSF, CTs appeared as either single events or bursts of two–five or more

events (Fig. 1B). Bursts of CTs were only occasionally observed in $Mg^{2+}$-containing ACSF.

As a population of SRIs exhibited complete silence during the 10-min recording in $Mg^{2+}$-containing ACSF (Table 1), the data were analyzed using two methods to detect any potential effect of subsequent pharmacological treatments. In the first one, we used a $2 \times 2$ contingency table with outcomes of 'CT present' or 'CT absent' in control and treatment groups. In the second method, the mean ± S.E.M. frequency of CTs was compared between control and treatment groups.

### 3.2. Effect of nAChR antagonists on CT frequency in SRI

As referred to in Section 1, the majority of SRIs express functional somatodendritic α7 nAChRs, whereas only approximately 25% of these neurons express functional α4β2 nAChRs [25]. In addition, most SRIs receive glutamatergic inputs that can be stimulated by activation of α3β4β2 nAChRs. Therefore, we examined the effects of the α7 nAChR antagonist MLA (10 nM) and the α3β4β2 nAChR antagonist mecamylamine (3 μM) on the frequency of CTs recorded from CA1 SRIs. The selected concentrations of these drugs had minimal interaction with other nAChR subtypes [15].

In the first set of experiments, we recorded spontaneous CTs in $Mg^{2+}$-containing ACSF under control condition for 15 min, during bath application of MLA (10 nM) for an additional 15 min, and, then, during wash with control ACSF. In two of seven SRIs (29% of cells), we observed a reversible decrease in the frequency of CTs (Fig. 2A). In the next set of experiments, to allow full equilibrium of the nAChRs with the antagonist, slices were first incubated with MLA (10 nM) for >1 h and subsequently transferred to the recording chamber containing ACSF with the same concentration of MLA. The CT frequency recorded from neurons of MLA-incubated slices and control slices were then compared. The percentage of SRIs from which CTs could be recorded and the frequency of CTs were not significantly affected by incubation of the slices with MLA (Table 1 and Fig. 2B). Similar results were obtained when CTs were recorded continuously for another 30 min during superfusion of the control and the MLA-incubated slices with $Mg^{2+}$-free ACSF without or with MLA, respectively (Fig. 2C).

In another set of experiments, we analyzed the effects of 3 μM mecamylamine on the number of SRIs from which CTs could be recorded and on the frequency of CTs. The percentage of SRIs from which CTs could be recorded was not affected by mecamylamine (Table 1). However, the frequency of CTs recorded from neurons in slices under control conditions was significantly higher than that recorded in the continuous presence of mecamylamine from neurons in slices that had been pre-incubated for >1 h in ACSF containing mecamylamine (Fig. 3A). Similar results were observed when CTs were recorded from neurons during superfusion of the control and the mecamylamine-incubated slices with $Mg^{2+}$-free ACSF without or with mecamylamine, respectively (Fig. 3B).

### 3.3. Effect of glutamate receptor antagonists on CT frequency in SRIs

Incubation of the hippocampal slices with ACSF containing the AMPA/kainate receptor antagonist CNQX (10 μM) had no effect on the frequency of CTs recorded from CA1 SRIs in the presence or in the absence of $Mg^{2+}$ (Fig. 4A and C). In contrast, incubation of the hippocampal slices with APV (50 μM)-containing ACSF resulted in a marked reduction of the number of neurons presenting spontaneous CTs and a significant suppression of CT frequency. While spontaneous CTs could be recorded from approximately 70% of the neurons studied in the absence of APV, no more than ca. 22% of the neurons studied in the presence of APV presented CTs ($p < 0.01$ by Fisher's exact test) (Table 1). In addition, the frequency of CTs recorded in the continuous presence of APV from neurons in hippocampal slices that had been incubated >1 h in APV-containing ACSF was significantly lower than that recorded from neurons in slices maintained in APV-free ACSF (Fig. 4B). Similar results were obtained when the ACSF used to perfuse the slices had no added $Mg^{2+}$.

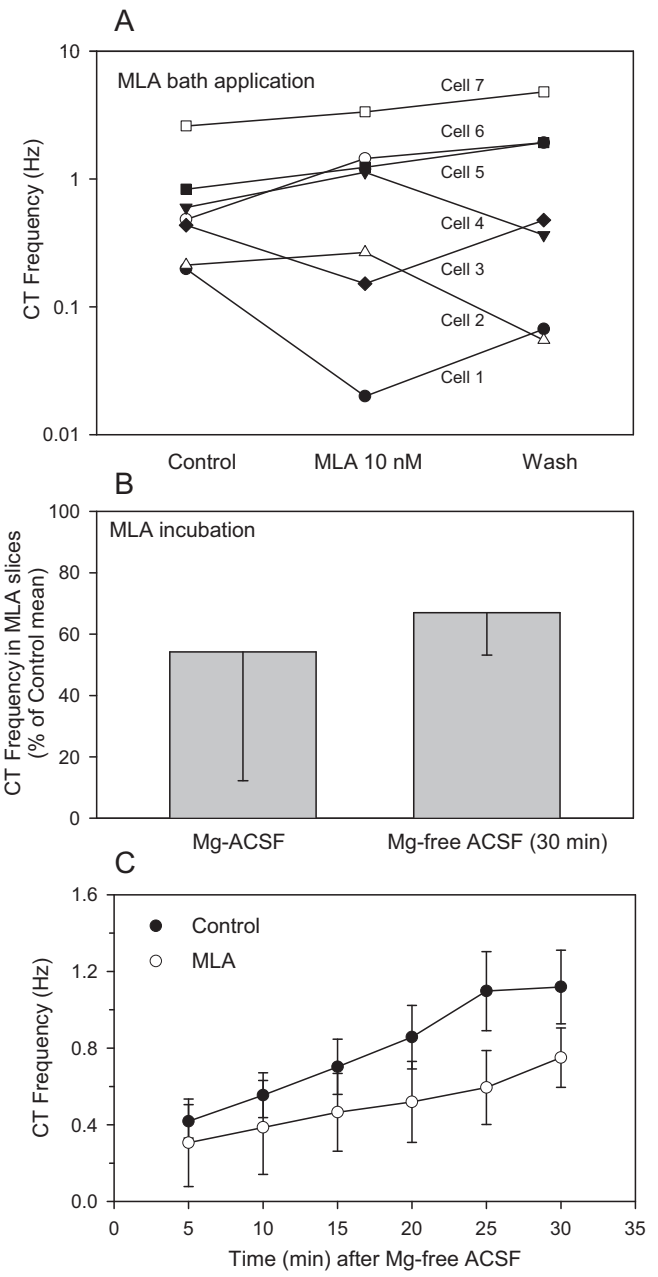


**Fig. 2.** Effect of MLA on CT frequency recorded from CA1 SRIs. A. Graph depicts the average frequency of CTs observed in each SRI under control condition ($Mg^{2+}$-containing ACSF, 10 min), during 5–15 min bath exposure to 10 nM MLA, and during 10–40 min wash with MLA-free ACSF. Only cell #1 and cell #3 revealed a reversible decrease of CT frequency by MLA bath application. B. Graph depicts the frequency of CTs recorded in the continuous presence of 10 nM MLA from several SRIs in MLA (10 nM)-incubated slices and normalized to the mean frequency of CTs recorded from neurons in control slices (i.e., slices incubated in MLA-free ACSF). Graph and error bars represent mean and S.E.M., respectively, of results obtained from 13 neurons. C. Time course of increase in the frequency of CTs recorded from the same neurons as in B during their superfusion with $Mg^{2+}$-free ACSF. Data points and error bars represent mean and S.E.M., respectively, of results obtained from 13 neurons in the MLA group and 58 neurons in the control group.

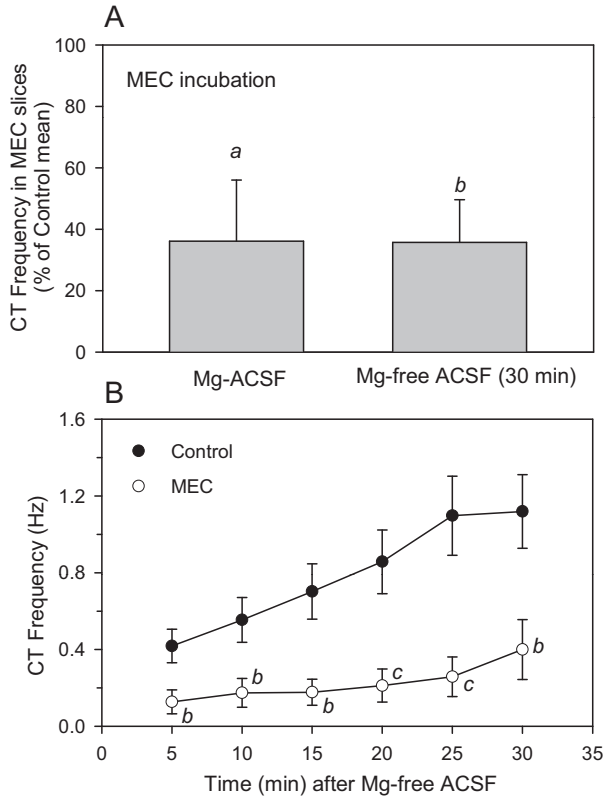


**Fig. 3.** Effect of mecamylamine on CT frequency recorded from CA1 SRIs. A. Graph depicts the frequency of CTs recorded in the continuous presence of mecamylamine (3 μM) from several SRIs in mecamylamine (3 μM)-incubated slices and normalized to the mean frequency recorded from neurons in control slices incubated in ACSF free of mecamylamine. Graph and error bars represent mean and S.E.M., respectively, of results obtained from nine neurons. B. Time course of increase in the frequency of CTs recorded from the same neurons as in A during their superfusion with $Mg^{2+}$-free ACSF. Data points and error bars represent mean and S.E.M., respectively of results obtained from nine neurons in the mecamylamine group and 58 neurons in the control group. a $p < 0.05$; b $p < 0.01$; c $p < 0.001$ compared to respective control by unpaired t-test.

### 3.4. Effect of exogenous and endogenous KYNA on CT frequency in the SRI

The frequency of CTs recorded from neurons following >1-h incubation of the hippocampal slices with KYNA-containing ACSF was significantly lower than that recorded under control conditions (Figs. 5 and 6). In an SRI of control hippocampal slices where spontaneous CTs appeared primarily as bursts in $Mg^{2+}$-free ACSF (see Cell 1 in Fig. 5), CT bursts disappeared within 3 min of the start of bath application of KYNA (200 μM). The bursts reappeared after a 5–10 min wash with control $Mg^{2+}$-free ACSF (third sample recording from top in Fig. 5A1). The source of CT bursts was explored using whole-cell patch configuration in the same SRI (Fig. 5A2). Under the whole-cell configuration, the SRI exhibited bursts of overlapping EPSCs that had slow decay kinetics characteristic of NMDA receptor activation. The number of EPSC bursts observed in the whole-cell configuration matched roughly the number of CT bursts recorded in the cell-attached configuration. At 2 min following the beginning of a second bath application of KYNA, the amplitude of the EPSC bursts decreased to roughly 60% of that of control EPSC bursts, and at 3 min no more EPSCs could be detected in the neuron (Fig. 5A2). The inhibitory effect of KYNA on the EPSCs reversed within 5 min of wash of the slices with $Mg^{2+}$-free ACSF containing no KYNA (Fig. 5A2). These EPSC bursts were also eliminated when the SRI was superfused with $Mg^{2+}$-containing ACSF (Fig. 5A2). In another control SRI where the

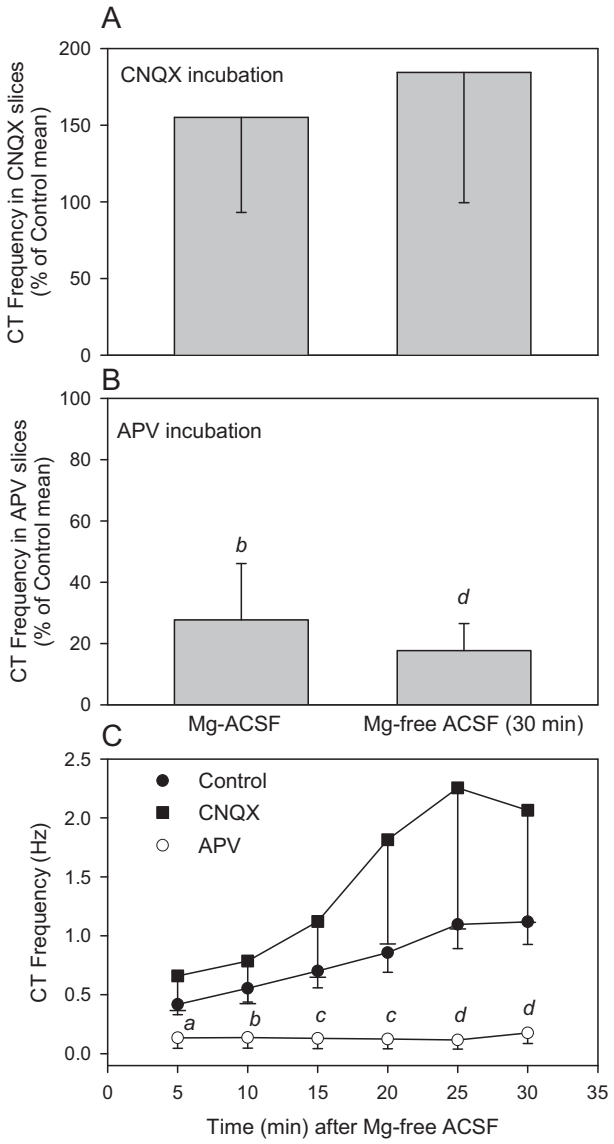


**Fig. 4.** Effect of CNQX and APV on CT frequency in CA1 SRI of rat hippocampal slices. A. Graph depicts the frequency of CTs recorded in the continuous presence of CNQX (10 μM) from several SRIs in CNQX (10 μM)-incubated slices and normalized to the mean frequency of CTs recorded from neurons in control slices incubated in ACSF free of CNQX. B. Graph depicts the frequency of CTs recorded in the continuous presence of APV (50 μM) from several SRIs in APV (50 μM)-incubated slices and normalized to the mean frequency of CTs recorded from neurons in control slices incubated in ACSF free of APV. Graph and error bars in A and B represent mean and S.E.M., respectively, of results obtained from 13 neurons incubated with CNQX and 9 neurons incubated with APV. C. Time-dependent changes in the frequency of CTs recorded from the same neurons as in A and B during their superfusion with $Mg^{2+}$-free ACSF are shown. Data points and error bars represent mean and S.E.M., respectively of results obtained from 13 neurons in the CNQX group, 9 neurons in the APV group, and 58 neurons in the control group. a $p < 0.05$; b $p < 0.01$; c $p < 0.001$; d $p < 0.0001$ compared to respective control by unpaired t-test.

spontaneous CTs consisted of both bursts and isolated events in $Mg^{2+}$-free ACSF (see Cell 2 in Fig. 5B), bath application of KYNA (200 μM) for 10 min abolished selectively the CT bursts, which then reappeared after a 10 min wash with control $Mg^{2+}$-free ACSF. These findings indicate that (i) NMDA receptor-mediated EPSC bursts trigger CT bursts in the SRIs, and (ii) KYNA (200 μM) abolishes CTs in SRIs predominantly via its action on NMDA receptors located on pyramidal neurons that synapse onto the interneurons and partly via block of NMDA receptors on the SRIs.

When hippocampal slices were incubated for >1 h in ACSF containing 2 μM KYNA, there was a marked reduction of the

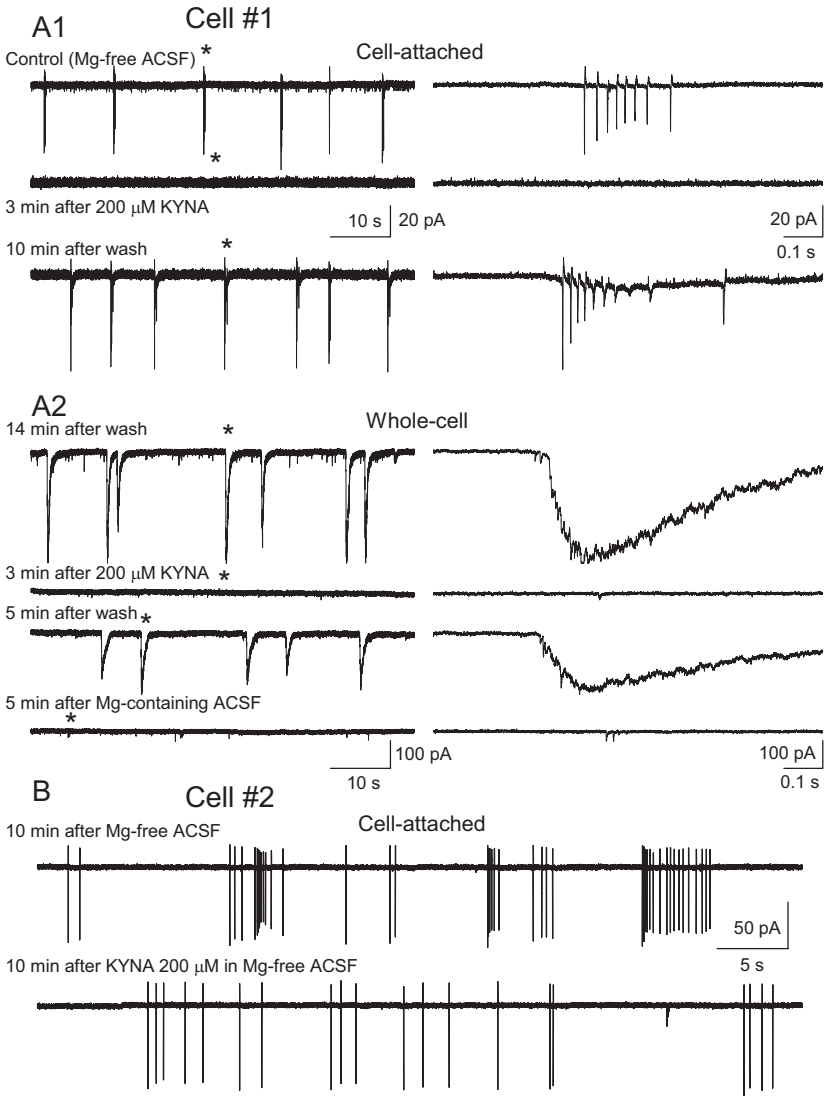


**Fig. 5.** Effect of high concentration of KYNA on the frequency of CTs and EPSCs in CA1 SRI of rat hippocampal slices. Sample recordings illustrate that brief bath application of 200 μM KYNA abolishes bursts of CTs and EPSCs recorded from an SRI in $Mg^{2+}$-free ACSF. A1. Representative traces of cell-attached recordings from an SRI under control condition, 3 min after bath applied KYNA (200 μM), and 10 min after wash with $Mg^{2+}$-free ACSF. The regions marked by asterisks are shown in an expanded scale to the right to reveal individual events in a single burst of CTs. Note the fast onset and reversal of inhibition. A2. Representative traces of whole-cell recordings at −60 mV from the same SRI as in A1 under control (i.e., during wash in $Mg^{2+}$-free ACSF), 3 min after bath applied KYNA (200 μM), 5 min wash in $Mg^{2+}$-free ACSF, and 5 min after exposure to $Mg^{2+}$-containing ACSF. The regions marked by asterisks are shown in an expanded scale to the right to reveal overlapping EPSCs in each burst. Note that the number of EPSC bursts matched the number of CT bursts and that a brief exposure (<3 min) to KYNA (200 μM) abolished both types of events completely. B. In another SRI, cell-attached recordings reveal the presence of CTs as both isolated events and bursts in $Mg^{2+}$-free ACSF. Bath application of KYNA (200 μM) predominantly abolished CT bursts in this cell.

frequency of spontaneous CTs recorded in the presence of $Mg^{2+}$ (Fig. 6A1 and A2). In addition, only 8% of the neurons incubated in 2 μM KYNA-containing ACSF exhibited CTs; this value is significantly different from control (Table 1). When control and KYNA (2 μM)-incubated slices were superfused with $Mg^{2+}$-free ACSF without or with KYNA (2 μM), respectively, the mean frequency of CTs recorded in the continuous presence of KYNA (2 μM) remained significantly lower than that recorded from neurons in the absence of KYNA up to 25 min from the beginning of the removal of extracellular $Mg^{2+}$. After 25 min in $Mg^{2+}$-free ACSF, however, the frequency of CTs recorded from neurons in the presence of 2 μM KYNA became comparable to that recorded in the absence of KYNA.

To examine the effect of endogenously produced KYNA on the frequency of CTs, slices were incubated in ACSF containing 200 μM kynurenine, which has been shown to enhance the de novo synthesis of endogenous KYNA in hippocampal slices [26]. In situ concentrations of KYNA produced from 200 μM kynurenine have been shown to be sufficient to inhibit α7 nAChRs and tonically active NMDA receptors, but not synaptic NMDA receptors [26].

Incubation with kynurenine reduced the number of cells exhibiting CTs to a significant extent (Table 1) and also suppressed to a significant extent the frequency of CTs recorded from neurons in slices superfused with $Mg^{2+}$-containing ACSF (Fig. 6B1 and B2). These results are consistent with the notion that KYNA-induced inhibition of tonically active NMDA receptors on CA1 SRIs decreases the excitability of these neurons. No significant inhibitory effect of kynurenine was observed in $Mg^{2+}$-free ACSF throughout the 30-min recording time (Fig. 6B2 and B3). This finding is in agreement with the previous demonstration that kynurenine (200 μM)-derived KYNA has no significant effect on synaptically active NMDA receptors [26], which, in the absence of $Mg^{2+}$, impart a powerful excitatory drive onto the CA1 SRIs.

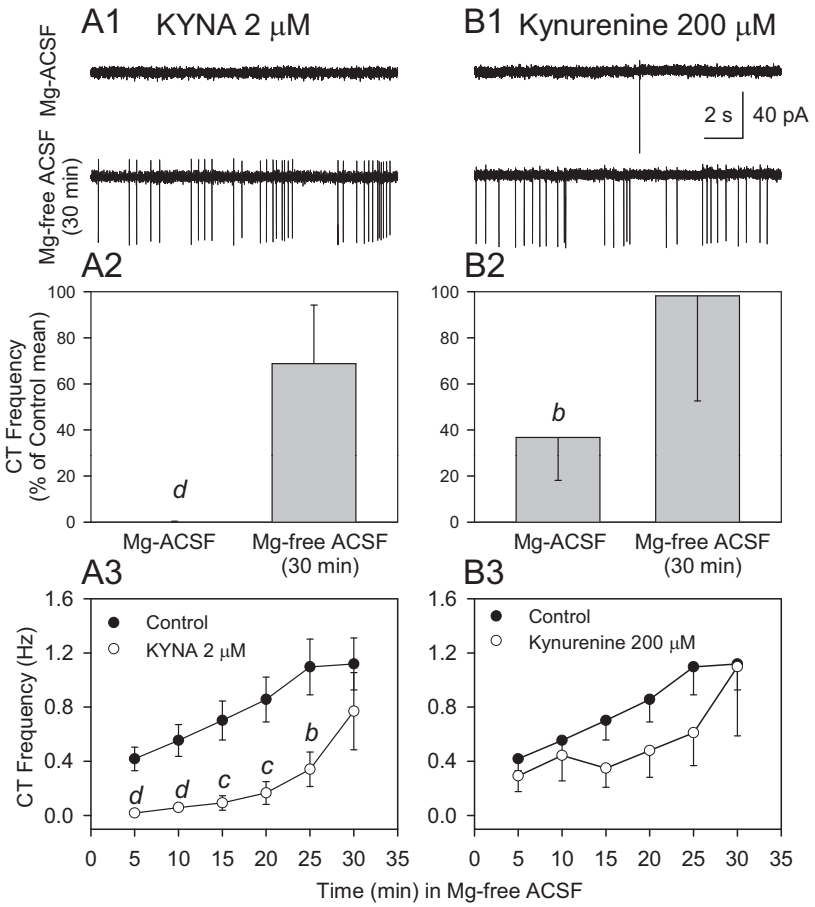


**Fig. 6.** Effect of kynurenine and low concentrations of KYNA on the frequency of CTs in CA1 SRIs. A1. Sample traces of cell-attached recordings in slices incubated with 2 μM KYNA in the presence and in the absence of added $Mg^{2+}$ in the ACSF. A2. Graph depicts the frequency of CTs recorded in the continuous presence of 2 μM KYNA from several SRIs in KYNA (2 μM)-incubated slices and normalized to the mean frequency recorded from neurons in control slices incubated in KYNA-free ACSF. A3. Time-dependent changes in the frequency of CTs recorded from the same neurons as in A2 during their superfusion with $Mg^{2+}$-free ACSF are shown. Data in A2 and A3 are presented as mean and S.E.M. of results obtained from 12 neurons in the KYNA group and 58 neurons in the control group. B1. Sample traces of cell-attached recordings in slices incubated with 200 μM kynurenine in $Mg^{2+}$-free and $Mg^{2+}$-containing ACSF. B2. Graph depicts the frequency of CTs recorded in the continuous presence of 200 μM kynurenine from several SRIs in kynurenine (200 μM)-incubated slices and normalized to the mean frequency recorded from neurons in control slices incubated in kynurenine-free ACSF. B3. Time-dependent changes in the frequency of CTs recorded from the same neurons as in B2 during their superfusion with $Mg^{2+}$-free ACSF are shown. Data in B2 and B3 are presented as mean and S.E.M. of results obtained from 22 neurons in ACSF containing $Mg^{2+}$ and kynurenine, 13 neurons in $Mg^{2+}$-free ACSF containing kynurenine, and 58 control neurons. b $p < 0.01$; c $p < 0.001$; d $p < 0.0001$ compared to respective control by unpaired t-test.

### 3.5. Effect of KYNA and APV on AMPA EPSCs

To gather insights on the mechanisms underlying the actions of KYNA on CTs, we analyzed the effects of 2 and 100 μM KYNA on the frequency of spontaneous AMPA EPSCs recorded from SRIs under whole-cell configuration. In our previous study, we reported that at high micromolar concentrations (100–200 μM) KYNA produces a significant decrease in the mean frequency and mean peak amplitude of AMPA EPSCs recorded from SRIs [26]. Here, we observed that at 2 μM KYNA has no significant effect on the mean frequency and mean peak amplitude of AMPA EPSCs (Frequency = 0.667 ± 0.165 Hz in control vs. 0.460 ± 0.133 Hz in KYNA; peak amplitude = 18.5 ± 0.99 pA in control vs. 16.65 ± 1.48 pA in KYNA, $n = 6$ neurons). However, when the distribution of AMPA EPSC peak amplitudes was compared among control and KYNA- or APV-incubated slices, a clear concentration-dependent effect of KYNA emerged (Fig. 7). At 2 μM, KYNA significantly reduced the frequency of AMPA EPSCs with amplitudes higher than 20 pA, but smaller than 30 pA (Fig. 7). At 100 μM, KYNA equally reduced the frequency of events with amplitudes larger than 20, 25, or 30 pA (Fig. 7). The effect of 100 μM KYNA on the frequency of AMPA EPSCs was comparable to that of 50 μM APV.

## 4. Discussion

The present study was designed to assess the role of endogenous activity of nAChRs and glutamate receptors in controlling the excitability of CA1 SRIs, and the effects of KYNA on the excitability of these interneurons in the rat hippocampus. Using the cell-attached mode of the patch-clamp technique, we demonstrate for the first time that, in the absence of external stimulation, basal levels of ACh in hippocampal slices are sufficient to activate mecamylamine-sensitive α3β4β2 nAChRs, but not α7 nAChRs. Using this assay, we also provide evidence that, under the present experimental conditions, the excitability of CA1 SRIs is maintained in part by active α3β4β2 nAChRs on glutamatergic neurons/axons synapsing onto the interneurons and by synaptically and tonically active NMDA receptors. Given the low affinity of α7 nAChRs to ACh and choline, it is likely that our inability to detect the contribution of α7 nAChRs to the excitability of the SRIs was a result of the absence of the septal cholinergic neurons, which constitute the major cholinergic input to the hippocampus [8], in our preparation. Without these neurons and in the absence of electrical stimulation of the cholinergic fibers that remain in the hippocampus, basal levels of ACh and choline in the hippocampal

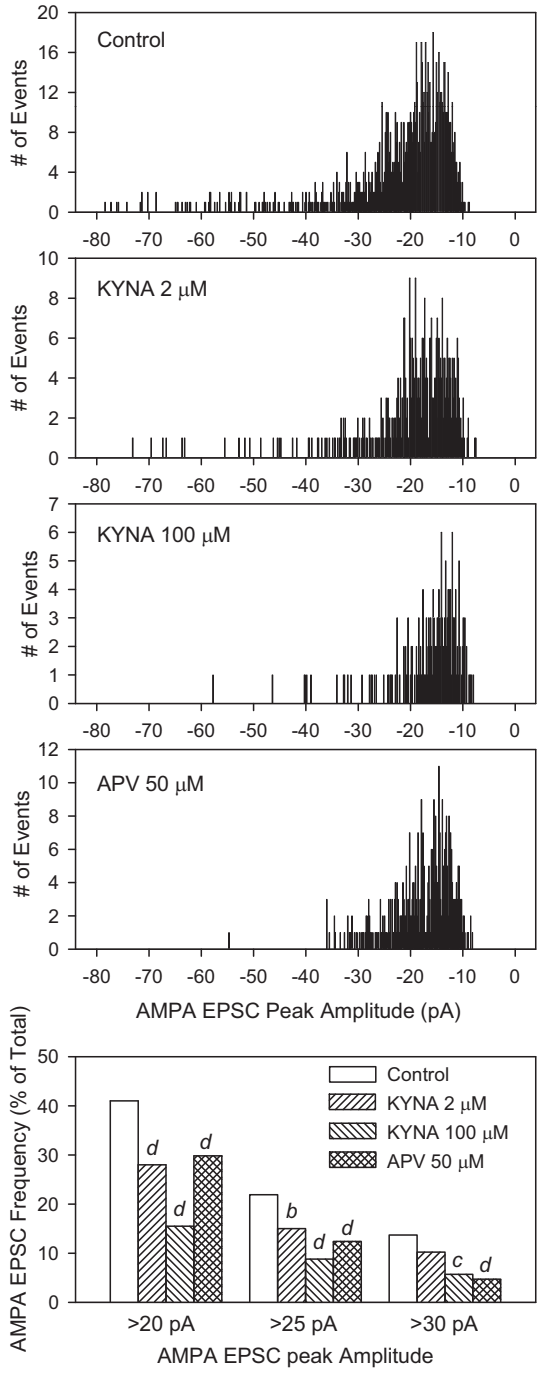


**Fig. 7.** Effect of KYNA on the amplitude distribution of AMPA EPSCs in CA1 SRI of hippocampal slices. Histograms of pooled data from several neurons reveal the distribution pattern of AMPA EPSC amplitudes recorded under different experimental conditions. Note that there are fewer large-amplitude events in the KYNA and APV groups compared to control. Bottom graph illustrates the relative frequency of large-amplitude AMPA EPSCs recorded under different experimental conditions. Number of events with threshold amplitudes of 20, 25 and 30 pA was normalized to the total number of events pooled under each experimental condition. About 60% of the events in the control group had amplitudes smaller than 20 pA. The percent value of the large-amplitude component in relation to the total number of events is significantly decreased by both concentrations of KYNA and by APV. b $p < 0.01$; c $p < 0.001$; d $p < 0.0001$, compared to control by Fisher's exact test. Results are from 1061 events pooled from 6 cells in control, 421 events pooled from 6 cells in 2 μM KYNA, 193 events pooled from 13 cells in 100 μM KYNA, and 403 events pooled from 5 cells in 50 μM APV.

slices would have been too low to cause sufficient activation of α7 nAChRs on the SRIs to induce neuronal firing. Finally, we report that at high micromolar concentrations KYNA, acting primarily as an NMDA receptor antagonist, decreases the excitability of CA1 SRIs. At low micromolar concentrations KYNA, acting via NMDA receptor-independent mechanisms, decreases the rate of firing of these interneurons. The significance of these findings is discussed below.

### *4.1. Relevance of CT frequency measurements and methodological considerations*

Action potentials are discrete, all-or-none units of electrical activity that transfer information between neurons in the brain. Neurons initiate and send electrical impulses as single units or multiple units that can be experimentally assessed as single or bursts of action potentials. Here, using cell-attached configuration, we assessed spontaneous firing of SRIs in the form of CTs, rather than action potentials. Although the conventional whole-cell current-clamp recording has the advantages of detecting spike amplitude and other parameters in addition to the frequency of action potentials, cell-attached recordings of CTs are simple and offer their own advantages. For example, in the cell-attached recordings, the neuron remained intact. Therefore, the absence of cell dialysis kept the intracellular ionic composition in its native state, maintained vital energy-dependent mechanisms, and preserved G-protein-coupled mechanisms, all of which have a direct bearing on neuronal excitability. Additionally, the recordings remained stable for >45 min and free of background noise, factors that were necessary to complete the long experimental protocols.

Although intrinsic activity, which relies on voltage-gated channels, can generate CTs in pyramidal neurons, chemical synaptic transmission operating via various neurotransmitter-gated ion channels remains the most effective and reliable mode to induce CTs in the interneurons in hippocampal slices [21,22]. The interaction of a neurotransmitter with a given receptor can induce, increase, or decrease the frequency of CTs depending on whether it causes depolarization or hyperpolarization. Thus, an analysis of the effects of receptor-selective agonists and antagonists on the frequency of CTs in a neuron can reveal how the activity of a given receptor-subtype contributes to the rate of firing of the neurons.

### *4.2. Tonically and synaptically active NMDA receptors regulate CA1 SRI excitability*

Results presented here suggest that tonically and synaptically active NMDA receptors have a critical role in the maintenance of neuronal firing. As expected, during exposure of the slices to $Mg^{2+}$-free ACSF, there was a time-dependent increase in the frequency of neuronal firing that could be accounted for by an increase in activity of both synaptic and extrasynaptic NMDA receptors on the SRIs due to a reduction of $Mg^{2+}$ block of these receptors [26]. The finding that APV suppressed predominantly large-amplitude AMPA EPSCs that typically result from action potential-driven glutamate release from presynaptic neurons (see Fig. 7) suggests that removal of extracellular $Mg^{2+}$ increased excitation of SRIs by enhancing the activity not only of NMDA receptors on the SRIs themselves but also on glutamate neurons/axons that synapse onto the SRIs.

### *4.3. Do endogenously active α7 nAChRs regulate the excitability of CA1 SRIs?*

CA1 SRIs express the highest number of α7 nAChRs among all the CA1 interneuron types [27]. Thus, CA1 SRIs are likely

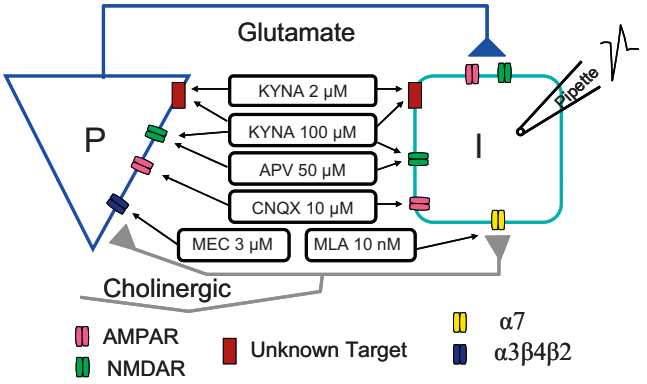


**Fig. 8.** Schematic representation of the putative neurocircuitry/receptors and targets likely to mediate the effects of the various pharmacological agents on CA1 SRI excitability in resting hippocampal slices. Axon from pyramidal neuron (P) releases glutamate, which, in turn activates AMPA and NMDA receptors on the SRIs (I) and lead to firing of action potentials. Lack of significant effect of MLA suggest that either the number of cholinergic synapses targeting α7 nAChRs on the SRIs is too low and/or that ACh-induced activation of α7 nAChR is too weak to initiate CT in the neurons. The potent inhibitory effect of mecamylamine suggests that basal levels of ACh in the hippocampal slices are sufficient to activate α3β4β2 nAChRs in glutamatergic neurons/axons that synapse onto the SRIs. The potent inhibitory effect of APV suggests that α3β4β2 nAChR activation by endogenous ACh may act in conjunction with NMDA receptor activation on both the SRIs themselves and the glumatergic neurons that synapse onto these interneurons to control the excitability of the latter. High concentration of KYNA inhibits NMDA receptors on both pyramidal neuron and SRIs to suppress SRI excitation. Low concentration of KYNA (2 μM), however, acts on an unknown target to reduce SRI excitability.

candidates to possess functional nicotinic cholinergic synapses operating via α7 nAChRs. Reports suggest the existence of α7 nAChR-mediated nicotinic transmission in the SRI [12,13] and other hippocampal interneurons [6]. However, synaptic transmission mediated by α7 nAChRs has only been detected in a small percentage of SRIs. If these nicotinic cholinergic synapses are active under resting conditions, as demonstrated by the presence of spontaneous nicotinic synaptic potentials in the hippocampal slices [6], and diffusing ACh and/or choline reach levels sufficiently high to activate non-synaptic α7 nAChRs, these receptors are likely to contribute to the resting excitability of SRIs in the slices. The lack of significant inhibition of CT frequency by MLA shown here suggests that, under resting conditions, basal levels of ACh/choline in the hippocampal slices are not sufficient to trigger SRI firing via activation of α7 nAChRs on the interneurons. It is possible that this mechanism would have been detected if the cholinergic fibers remaining in the hippocampal slices had been electrically stimulated or in a septal-hippocampal slice preparation in which the major cholinergic input to the hippocampus would have been intact. Alternatively, the α7 nAChRs present on the SRIs may have roles other than simply mediating excitation of the neurons [15].

### 4.4. Endogenously active α3β4β2 nAChRs regulate SRI excitability

Exogenous activation of α3β4β2 nAChRs has been shown to trigger release of glutamate that, in turn, activates both AMPA and NMDA receptor-mediated EPSCs on SRIs and, consequently, increases the rate of firing of these neurons [20]. To date, it was unknown whether endogenously released ACh reach levels sufficient to activate α3β4β2 nAChRs and produce excitation of SRIs in the hippocampal slices. The results presented in Fig. 3 demonstrate unequivocally the involvement of α3β4β2 nAChRs in controlling the resting excitability of SRI. We propose that endogenous levels of ACh in the hippocampal slices are sufficient to activate α3β4β2 nAChRs on glutamate neurons/axons that synapse onto the CA1 SRIs. Activation of these nAChRs leads to release of glutamate that, in turn, activates AMPA and NMDA receptors on the SRIs leading to the depolarization of these neurons and increasing their excitability.

### 4.5. Mechanisms of action of KYNA in suppressing SRI excitability

High micromolar concentrations of KYNA produced a rapid and reversible inhibition of CTs via NMDA receptor blockade (Figs. 5 and 8). Interestingly, KYNA-induced block of NMDA receptors must have occurred at both glutamate neurons/axons synapsing onto the SRIs and on the SRIs themselves. Two lines of evidence suggest that the effect of KYNA on CTs result primarily from a presynaptic action. First, we observed that the EPSC bursts ceased abruptly during exposure to 200 μM KYNA (Fig. 5), a result inconsistent with an exclusive postsynaptic blockade, which would have led to a gradual reduction in the amplitude of EPSCs. Second, 100–200 μM KYNA reduced the frequency more than the peak amplitude of AMPA EPSCs [26], and 100 μM KYNA selectively suppressed large-amplitude AMPA EPSCs, which normally reflect action potential-driven activity in the presynaptic pyramidal neurons.

Most dramatic decrease in the frequency of CTs was observed with low micromolar concentration of KYNA (i.e., 2 μM). It is unlikely that NMDA receptor blockade is involved here because 2 μM KYNA was found to be more effective than the NMDA receptor blocker APV in reducing the CT frequency (compare Figs. 4 and 6). Besides, this concentration of KYNA is well below that needed to block NMDA receptors. The effective concentration of KYNA that inhibits 50% of NMDA-evoked responses ranges between 15 μM in the absence of glycine and 235 μM in presence of glycine [4]. It is also unlikely that α7 nAChRs are involved because full blockade of α7 nAChRs using 10 nM MLA failed to produce significant inhibition of CT frequency (Fig. 2). This implies that low micromolar concentration of KYNA acts at a site other than NMDA receptors and α7 nAChRs. Although the precise mechanism of action of low micromolar concentrations of KYNA remains to be identified, one can speculate that KYNA acting via G-protein-coupled metabotropic receptors and/or potassium channels produced hyperpolarization of SRIs and thereby suppressed the CTs. The orphan receptor GPR35 is unlikely to be the target because only at high micromolar concentrations do KYNA inhibit this receptor [28,29]. Based on the observation that 2 μM KYNA suppresses predominantly large-amplitude AMPA EPSCs (Fig. 7), we can suggest that low micromolar concentration of KYNA has an inhibitory action at the presynaptic pyramidal neurons (see Fig. 8). Such an action is consistent with the recent report that reduction of endogenous KYNA levels enhances glutamate levels in the hippocampus and the cerebral cortex [30,31].

Elevation of endogenous KYNA by incubation of slices with 200 μM kynurenine also had a suppressive effect on the CT frequency. However, significant inhibition was achieved only in $Mg^{2+}$-containing ACSF and not in $Mg^{2+}$-free ACSF (Fig. 6). It is possible that suppression of tonic NMDA currents in the SRI [26] by astrocyte-produced KYNA played a role in the CT suppressive effects of kynurenine. Kynurenine was less effective in suppressing CTs in $Mg^{2+}$-free ACSF unlike exogenously applied 2 μM KYNA. This difference could be explained by the fact that kynurenine incubation did not generate enough KYNA in the regions beyond its production/release sites. It is estimated that during exposure to 200 μM kynurenine the free extracellular concentration of KYNA in the incubation chamber was in the range of 50–200 nM between 2 and 6 h [26], and this concentration declines further during superfusion of the slices.

### 4.6. Pharmacological and clinical relevance

In the present study, the use of low micromolar concentrations of mecamylamine demonstrated that endogenously active non-α7

nAChRs present on glutamatergic axons/neurons that synapse onto CA1 SRIs contribute to the excitability of these interneurons. Since hippocampal network oscillations, which play an essential role in cognitive processing, rely upon the activity of GABAergic interneurons, it is tempting to speculate that mecamylamine-induced memory impairment observed in experimental animals [32] results in part from the reduced excitability of CA1 SRIs.

The reduced excitability of CA1 SRIs by low micromolar concentrations of KYNA may also be an important determinant of the sensory gating impairment that has been suggested to be secondary to deficient GABAergic transmission in the hippocampus of patients with schizophrenia [1].

In conclusion, we have demonstrated that, under resting conditions, endogenously active $\alpha3\beta4\beta2$ nAChRs as well as tonically and synaptically active NMDA receptors have a profound impact in maintaining the excitability of CA1 SRIs in rat hippocampal slices. Also, we have identified in the CA1 SRIs a novel inhibitory action of KYNA that cannot be explained on the basis of its effects on known targets such as $\alpha7$ nAChR and NMDA receptors.

## Acknowledgements

The authors are indebted to Mabel Zelle and Bhagavathy Alkondon for technical assistance. This work was supported by the National Institutes of Health National Institute of Neurological Disorders and Stroke [Grant NS25296, EXA].

## References

[1] Freedman R, Goldowitz D. Studies on the hippocampal formation: from basic development to clinical applications: studies on schizophrenia. Prog Neurobiol 2010;90:263–75.
[2] Schwarcz R, Rassoulpour A, Wu HQ, Medoff D, Tamminga CA, Roberts RC. Increased cortical kynurenate content in schizophrenia. Biol Psychiatry 2001;50:521–30.
[3] Alkondon M, Pereira EFR, Yu P, Arruda EZ, Almeida LEF, Guidetti P, et al. Targeted deletion of the kynurenine aminotransferase II gene reveals a critical role of endogenous kynurenic acid in the regulation of synaptic transmission via $\alpha7$ nicotinic receptors in the hippocampus. J Neurosci 2004;24:4635–48.
[4] Hilmas C, Pereira EFR, Alkondon M, Rassoulpour A, Schwarcz R, Albuquerque EX. The brain metabolite kynurenic acid inhibits $\alpha7$ nicotinic receptor activity and increases non-$\alpha7$ nicotinic receptor expression: pathophysiological implications. J Neurosci 2001;21:7463–73.
[5] Lopes C, Pereira EF, Wu HQ, Purushottamachar P, Njar V, Schwarcz R, et al. Competitive antagonism between the nicotinic allosteric potentiating ligand galantamine and kynurenic acid at $\alpha7^*$ nicotinic receptors. J Pharmacol Exp Ther 2007;322:48–58.
[6] Stone TW. Kynurenic acid blocks nicotinic synaptic transmission to hippocampal interneurons in young rats. Eur J Neurosci 2007;25:2656–65.
[7] Mesulam MM. The cholinergic innervation of the human cerebral cortex. Prog Brain Res 2004;145:67–78.
[8] Frotscher M. Cholinergic neurons in the rat hippocampus do not compensate for the loss of septohippocampal cholinergic fibers. Neurosci Lett 1988;87:18–22.
[9] Frotscher M, Vida I, Bender R. Evidence for the existence of non-GABAergic, cholinergic interneurons in the rodent hippocampus. Neuroscience 2000;96:27–31.
[10] Pitler TA, Alger BE. Cholinergic excitation of GABAergic interneurons in the rat hippocampal slice. J Physiol 1992;450:127–42.
[11] Stewart M, Fox SE. Do septal neurons pace the hippocampal theta rhythm? Trends Neurosci 1990;13:163–8.
[12] Alkondon M, Pereira EFR, Albuquerque EX. $\alpha$-Bungarotoxin- and methyllycaconitine-sensitive nicotinic receptors mediate fast synaptic transmission in interneurons of rat hippocampal slices. Brain Res 1998;810:257–63.
[13] Frazier CJ, Buhler AV, Weiner JL, Dunwiddie TV. Synaptic potentials mediated via $\alpha$-bungarotoxin-sensitive nicotinic acetylcholine receptors in rat hippocampal interneurons. J Neurosci 1998;18:8228–35.
[14] Wanaverbecq N, Semyanov A, Pavlov I, Walker MC, Kullmann DM. Cholinergic axons modulate GABAergic signaling among hippocampal interneurons via postsynaptic $\alpha7$ nicotinic receptors. J Neurosci 2007;27:5683–93.
[15] Albuquerque EX, Pereira EFR, Alkondon M, Rogers SW. Mammalian nicotinic acetylcholine receptors: from structure to function. Physiol Rev 2009;89:73–120.
[16] Alkondon M, Pereira EFR, Barbosa CT, Albuquerque EX. Neuronal nicotinic acetylcholine receptor activation modulates gamma-aminobutyric acid release from CA1 neurons of rat hippocampal slices. J Pharmacol Exp Ther 1997;283:1396–411.
[17] Alkondon M, Albuquerque EX. Nicotinic acetylcholine receptor $\alpha7$ and $\alpha4\beta2$ subtypes differentially control GABAergic input to CA1 neurons in rat hippocampus. J Neurophysiol 2001;86:3043–55.
[18] Jones S, Yakel JL. Functional nicotinic ACh receptors on interneurones in the rat hippocampus. J Physiol 1997;504:603–10.
[19] McQuiston AR, Madison DV. Nicotinic receptor activation excites distinct subtypes of interneurons in the rat hippocampus. J Neurosci 1999;19:2887–96.
[20] Alkondon M, Pereira EFR, Albuquerque EX. NMDA and AMPA receptors contribute to the nicotinic cholinergic excitation of CA1 interneurons in the rat hippocampus. J Neurophysiol 2003;90:1613–25.
[21] Khazipov R, Leinekugel X, Khalilov I, Gaiarsa J-L, Ben-Ari Y. Synchronization of GABAergic interneuronal network in CA3 subfield of neonatal rat hippocampal slices. J Physiol 1997;498:763–72.
[22] Cohen I, Miles R. Contributions of intrinsic and synaptic activities to the generation of neuronal discharges in in vitro hippocampus. J Physiol 2000;524:485–502.
[23] Stuart G, Schiller J, Sakmann B. Action potential initiation and propagation in rat neocortical pyramidal neurons. J Physiol 1997;505:617–32.
[24] Williams SR, Stuart GJ. Mechanisms and consequences of action potential burst firing in rat neocortical pyramidal neurons. J Physiol 1999;521:467–82.
[25] Alkondon M, Albuquerque EX. Nicotinic receptor subtypes in rat hippocampal slices are differentially sensitive to desensitization and early in vivo functional up-regulation by nicotine and to block by bupropion. J Pharmacol Exp Ther 2005;313:740–50.
[26] Alkondon M, Pereira EFR, Eisenberg HM, Kajii Y, Schwarcz R, Albuquerque EX. Age dependency of inhibition of $\alpha7$ nicotinic receptors and tonically active N-methyl-D-aspartate receptors by endogenously produced kynurenic acid in the brain. J Pharmacol Exp Ther 2011;337:572–82.
[27] Alkondon M, Aracava Y, Pereira EF, Albuquerque EX. A single in vivo application of cholinesterase inhibitors has neuron type-specific effects on nicotinic receptor activity in guinea pig hippocampus. J Pharmacol Exp Ther 2009;328:69–82.
[28] Wang J, Simonavicius N, Wu X, Swaminath G, Reagan J, Tian H, et al. Kynurenic acid as a ligand for orhphan G protein-coupled receptor GPR35. J Biol Chem 2006;281:22021–8.
[29] Guo J, Williams DJ, Puhl III HL, Ikeda SR. Inhibition of N-type calcium channels by activation of GPR35, an orphan receptor, heterologously expressed in rat sympathetic neurons. J Pharmacol Exp Ther 2008;324:342–51.
[30] Potter MC, Elmer GI, Bergeron R, Albuquerque EX, Guidetti P, Wu HQ, et al. Reduction of endogenous kynurenic acid formation enhances extracellular glutamate, hippocampal plasticity, and cognitive behavior. Neuropsychopharmacology 2010;35:1734–42.
[31] Konradsson-Geuken A, Wu HQ, Gash CR, Alexander KS, Campbell A, Sozeri Y, et al. Cortical kynurenic acid bi-directionally modulates prefrontal glutamate levels as assessed by microdialysis and rapid electrochemistry. Neuroscience 2010;169:1848–59.
[32] Levin ED, Bradley A, Addy N, Siqurani N. Hippocampal alpha7 and alpha4 beta 2 nicotinic receptors and working memory. Neuroscience 2002;109:757–65.